Performance analysis of continuous-variable measurement-device-independent quantum key distribution under diverse weather conditions*

Shu-Jing Zhang(张淑静)[1], Chen Xiao(肖晨)[2], Chun Zhou(周淳)[1], Xiang Wang(汪翔)[1], Jian-Shu Yao(要建姝)[3], Hai-Long Zhang(张海龙)[1,†], and Wan-Su Bao(鲍皖苏)[1]

[1] *Henan Key Laboratory of Quantum Information and Cryptography, PLA SSF IEU, Zhengzhou* 450001, *China*
[2] *PLA SSF IEU, Zhengzhou* 450001, *China*
[3] *Fujian Chengyi College of Jimei University, Xiamen* 361021, *China*

(Received 17 August 2019; revised manuscript received 13 November 2019; accepted manuscript online 5 December 2019)

The effects of weather conditions are ubiquitous in practical wireless quantum communication links. Here in this work, the performances of atmospheric continuous-variable measurement-device-independent quantum key distribution (CV-MDI-QKD) under diverse weather conditions are analyzed quantitatively. According to the Mie scattering theory and atmospheric CV-MDI-QKD model, we numerically simulate the relationship between performance of CV-MDI-QKD and the rainy and foggy conditions, aiming to get close to the actual combat environment in the future. The results show that both rain and fog will degrade the performance of the CV-MDI-QKD protocol. Under the rainy condition, the larger the raindrop diameter, the more obvious the extinction effect is and the lower the secret key rate accordingly. In addition, we find that the secret key rate decreases with the increase of spot deflection distance and the fluctuation of deflection. Under the foggy condition, the results illustrate that the transmittance decreases with the increase of droplet radius or deflection distance, which eventually yields the decrease in the secret key rate. Besides, in both weather conditions, the increase of transmission distance also leads the secret key rate to deteriorate. Our work can provide a foundation for evaluating the performance evaluation and successfully implementing the atmospheric CV-MDI-QKD in the future field operation environment under different weather conditions.

Keywords: weather conditions, atmospheric continuous-variable measurement-device-independent quantum key distribution (CV-MDI-QKD), performance

PACS: 03.67.Dd, 03.67.Hk, 03.67.–a **DOI:** 10.1088/1674-1056/ab5efd

1. Introduction

A complete system of military communication is the basis for winning over future informationalized wars. As one of the vital communication methods, quantum key distribution (QKD)[1–5] has matured to commercial and military applications. In relatively ideal conditions, a great many of QKD protocols have been implemented through optical fibers channels or atmospheric channels. A model of atmospheric CV-QKD has been established.[6] Backgroung noise of satellite-to-ground quantum key distribution has been investigated.[7] Low orbit satellite quantum communication has been designed and analyzed.[8] However, in the future battlefields, atmospheric QKD is a fairly better option, due to the fact that the relatively complex environment will make the optical fibers channels difficult to be laid down and easy to be destroyed. When implementing the QKD protocol in atmospheric channel, the quantum states are inevitably affected by atmospheric turbulence,[9–12] rain, fog, and other factors of natural environment,[13,14] which mainly from the absorption and scattering of light.

The continuous-variable measurement-device-independent quantum key distribution (CV-MDI-QKD)[15–18] is a great protocol, which is proposed to solve the flaw of detector imperfection. In fact, as a relatively flexible deployment, the CV-MDI-QKD is closer to the battlefield. However, there have been conducted quite a few studies of the transmission of CV-MDI-QKD in the atmosphere so far. The CV-MDI-QKD via satellite and atmosphere has been investigated.[19,20] The rain and fog are the key weather factors, which can influence the implementation of atmospheric CV-MDI-QKD protocol. When we study atmospheric CV-MDI-QKD in rain and fog environment, we must consider these two key factors. However, the corresponding research on transmission of CV-MDI-QKD protocol is still incomplete.

In the environment of rainfall and fog, the extinction effect of raindrops and fog droplets on the absorption and scattering of light are the main factors affecting the optical quantum transmission.[21] Therefore, in this paper, According to the Mie scattering theory[22–25] and the beam deflection model, we study the effect of rain and fog on the CV-MDI-QKD protocol. Hence, we establish and simulate the relationship between raindrop diameter, radius of fog droplet and the

*Project supported by the National Natural Science Foundation of China (Grant No. 61505261).
†Corresponding author. E-mail: zhhl049@126.com

secret key rate of protocol, which provides a theoretical basis for the normal operation of CV-MDI-QKD protocol in the atmosphere of rainfall and fog. In addition, when the beam arrives at the receiving telescope, the deflection and broadening phenomenon will occur,[26] which also leads the signal to attenuate. We also introduce this attenuation of CV-MDI-QKD. Meanwhile, the effects of transmission distance is also considered.

The rest of this paper is organized as follows. In Section 2, the CV-MDI-QKD in atmospheric environment is introduced. In Section 3, the secret key rate of the CV-MDI-QKD in the rain and deflection model is derived and numerically simulated. In Section 4, according to the characteristics of fog and Mie scattering theory, the CV-MDI-QKD model in atmospheric environment under foggy condition is established. Finally, some conclusions are drawn from the presnet study in Section 5.

2. Atmospheric CV-MDI-QKD model

In an actual intricate operation environment, both sides of communication need the support from untrustworthy third party to distribute secret keys. In order to adapt to the mutative environment, we assume that the third party is a satellite or a mobile aircraft, which is similar to CV-MDI-QKD model. Next, we will analyze the model of atmospheric CV-MDI-QKD, which is shown in Fig. 1.[18]

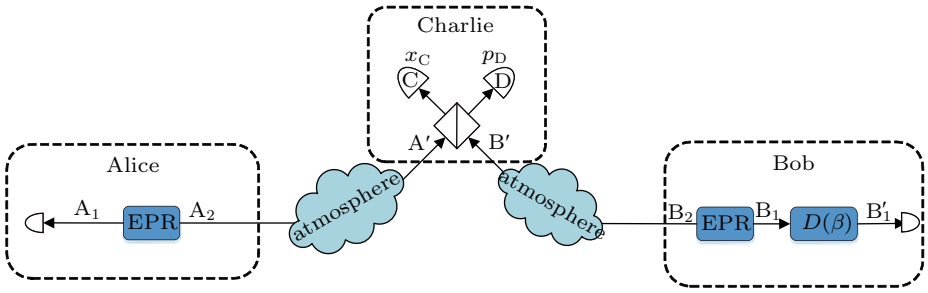

Fig. 1. Atmospheric CV-MDI-QKD model of communication between Alice and Bob via untrusted third party Charlie.

Two-mode squeezed vacuum states $\rho_{A_1A_2}$ and $\rho_{B_1B_2}$ are initially owned by Alice and Bob respectively. Assuming that two-mode squeezed state of Alice and Bob are both 0 for the mean value, the covariance matrix can be expressed as

$$\gamma = \begin{pmatrix} VI & \sqrt{V^2-1}Z \\ \sqrt{V^2-1}Z & VI \end{pmatrix}, \tag{1}$$

where $Z = \mathrm{diag}(1,-1)$, $I = \mathrm{diag}(1,1)$, and V is the Modulation variance. Keeping modes A_1 and B_1 on each side, they send the other modes A_2 and B_2 to the untrusted third party (Charlie) through two different atmospheric channels with transmissivities T_A and T_B. Assuming that the values of T_A and T_B are fixed, the received states at Charlie $\rho_{A_1A'}$ and $\rho_{B'B_1}$ are still Gaussian, and described in the following covariance matrix:[19]

$$\gamma_{A_1A'} = \begin{pmatrix} VI & \sqrt{T_A}\sqrt{V^2-1}Z \\ \sqrt{T_A}\sqrt{V^2-1}Z & (T_AV+(1-T_A)+\varepsilon_A)I \end{pmatrix},$$
$$\gamma_{B'B_1} = \begin{pmatrix} (T_BV+(1-T_B)+\varepsilon_B)I & \sqrt{T_B}\sqrt{V^2-1}Z \\ \sqrt{T_B}\sqrt{V^2-1}Z & VI \end{pmatrix}, \tag{2}$$

where ε_A and ε_B are the excess noise that is independent of channel.

The received modes A′ and B′ are swapped via a Bell's measurement at the Charlie. Charlie combines the two received modes A′ and B′ with a beam splitter, the output modes of the beam splitter are C and D. Then the new quadratures $\hat{x}_C = (1/\sqrt{2})(\hat{x}_{A'} - \hat{x}_{B'})$ and $\hat{p}_D = (1/\sqrt{2})(\hat{p}_{A'} + \hat{p}_{B'})$ are measured by two homodyne detectors, providing the classical outcome (x_C, p_D) with probability $p(x_C, p_D)$. The swapping process continues. Charlie transmits the Bell's measurements through a classical public channel to Alice and Bob. After receiving the Bell's measurements of Charlie, Bob displaces mode B_1 with B_1' by operation $D(\beta)$. Then Bob measures mode B_1' by using the homodyne detection, which randomly detects the x quadrature or p quadrature. Alice also measures mode A_1 to obtgain the final data. The covariance matrix of the conditional state $\rho_{A_1B_1'}$ shared between Alice and Bob is as follows:[19,20]

$$\gamma_{A_1B_1'} = \begin{pmatrix} VI & 0 \\ 0 & VI \end{pmatrix} - (V^2-1)\begin{pmatrix} \frac{T_A}{\theta}I & -\frac{\sqrt{T_AT_B}}{\theta}Z \\ -\frac{\sqrt{T_AT_B}}{\theta}Z & \frac{T_B}{\theta}I \end{pmatrix}, \tag{3}$$

where $\theta = (V-1)(T_A+T_B)+(\varepsilon_A+\varepsilon_B)+2$.

Once Alice and Bob have collected a sufficiently large amount of correlated data, they begin to perform a parameter estimation. Then Alice and Bob proceed with classical data post processing, information reconciliation and privacy amplification to distill a secret key.

The secret key rate K is given as[27]

$$K = \beta I_{AB} - \chi_{BE}, \tag{4}$$

where β is the reconciliation efficiency, I_{AB} is the Shannon mutual information of Alice and Bob, and χ_{BE} is the Holevo quantity, which can be expressed as[27]

$$\chi_{BE} = S(\rho_E) - S(\rho_{E|B}), \tag{5}$$

where $S(\rho_E)$ is the von Neumann entropy that Eve obtained, $S(\rho_{E|B})$ is the Eve's state conditional on Bob's measurement result.

Then, we should calculate I_{AB} and χ_{BE} in order to obtain the secret key rate. We can write $\gamma_{A_1B_1'}$ as

$$\gamma_{A_1B_1'} = \begin{pmatrix} (V - \dfrac{(V^2-1)T_A}{\theta})I & \dfrac{(V^2-1)(\sqrt{T_AT_B})}{\theta}Z \\ \dfrac{(V^2-1)(\sqrt{T_AT_B})}{\theta}Z & \left(V - \dfrac{(V^2-1)T_B}{\theta}\right)I \end{pmatrix}. \tag{6}$$

Then, $\gamma_{A_1B_1'}$ has the following form:

$$\gamma_{A_1B_1'} = \begin{pmatrix} AI & CZ \\ CZ & BI \end{pmatrix}. \tag{7}$$

Mutual information between Alice and Bob can be obtained by covariance matrix[19]

$$I_{AB} = \frac{1}{2}\log_2 \frac{A}{A - C^2/B}. \tag{8}$$

χ_{BE} can be shown as

$$\chi_{BE} = \sum_{i=1}^{2} G(\lambda_i) - G(\lambda_3), \tag{9}$$

where

$$G(x) = \left(\frac{x+1}{2}\right)\log_2\left(\frac{x+1}{2}\right) - \frac{x-1}{2}\log_2\left(\frac{x-1}{2}\right),$$

and λ_1, λ_2 are the symplectic eigenvalues of covariance matrix $\gamma_{A_1B_1'}$

$$\lambda_{1,2}^2 = \Delta \pm \sqrt{\Delta^2 - 4\det(\gamma_{A_1B_1'})}/2,$$

with $\Delta = A^2 + B^2 - 2C^2$, $\lambda_3^2 = A(A - C^2/B)$.[19]

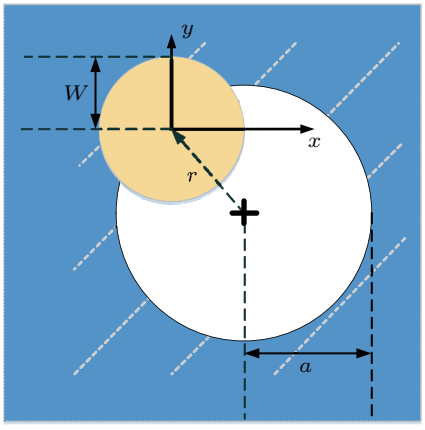

Fig. 2. Beam deflection, where circle with radius a is receiving plane, circle with radius W is receiving beam and r is distance of wandering.

The fluctuating atmospheric channel will cause a corresponding effect on the transmittance. The affected channel transmittance can be represented by T_1 with a probability density distribution of $P(T_1)$. In this paper, we first consider the beam deflection and distortion caused by atmospheric effect. The deviation of beam center from the receiver center is shown in Fig. 2, where a is the radius of receiver, W is the radius of beam, and r is the distance of wandering.

When the beam reaches the receiving plane, the center of the beam does not coincide with the center of the receiver, which results in deflection. Assuming that the beam fluctuates in the central plane of the receiver aperture. The probability density distribution can be expressed by Weibull distribution[26]

$$P(T_1) = \frac{2R^2}{\sigma^2 Q T_1}\left(2\ln\frac{T_0}{T_1}\right)^{2/Q-1} \times \exp\left(-\frac{1}{2\sigma^2}R^2\left(2\ln\frac{T_0}{T_1}\right)^{2/Q}\right), \tag{10}$$

where σ^2 is variance of wandering. The incomplete Weber integral is used in the transmission efficiency of beam[28]

$$T_1^2 = \frac{2}{\pi W^2}\mathrm{e}^{-2r^2/W^2}\int_0^a \mathrm{d}\rho\rho\,\mathrm{e}^{-2\rho^2/W^2} I_0\left(\frac{4}{W^2}r\rho\right), \tag{11}$$

where is the modified Bessel function. Incomplete Weber integral is defined as[28]

$$Q_n(x,z) = (2x)^{-n-1}\mathrm{e}^x\int_0^z \mathrm{d}t t^{n+1}\exp\left(-\frac{t^2}{4x}\right)I_n(t). \tag{12}$$

According to this definition, the transmission efficiency can be shown as[26]

$$T_1^2 = T_0^2\exp\left[-\left(\frac{r}{R}\right)^Q\right], \tag{13}$$

where T_0 is the maximum transmission efficiency for a given beam radius W, which can be expressed as[26]

$$T_0^2 = 1 - \exp\left(-2\frac{a^2}{W^2}\right). \tag{14}$$

We can use the same consideration to obtain the scale parameter R and shape parameter Q as follows:[26]

$$R = a\left[\ln\left(\frac{2T_0^2}{1-\exp(-4a^2/W^2)I_0(4a^2/W^2)}\right)\right]^{-1/Q}, \tag{15}$$

$$Q = 8\frac{a^2}{W^2}\frac{\exp(-4a^2/W^2)I_1(4a^2/W^2)}{1-\exp(-4a^2/W^2)I_0(4a^2/W^2)} \times \left[\ln\left(\frac{2T_0^2}{1-\exp(-4a^2/W^2)I_0(4a^2/W^2)}\right)\right]^{-1}. \tag{16}$$

Once the receiver is deployed, the size of the receiver aperture is determined. Therefore, the receiver aperture is considered

as an immutable value. In this paper, we set $a = 110$ mm simply. Figure 3 shows the relationship between the deflection distance and transmittance. The values of beam radius W are $0.2a$, a, and $2a$, respectively. It can be seen from Fig. 3 that (i) the larger the beam radius of the receiver, the smaller the transmittance is, (ii) with the increase of deflection distance, the transmittance decreases rapidly, (iii) The smaller the radius of the beam, the shorter the allowed deflection distance is and the faster the transmittance reaches 0.

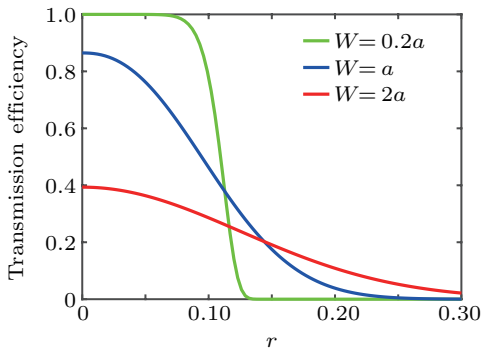

Fig. 3. Plots of transmittance *versus* beam wandering distance. Values of beam radius W are $0.2a$, a, and $2a$, respectively.

3. Effect of rain on atmospheric CV-MDI-QKD

Raining happens randomly in time and space, which is animportant factor of weather leading to a future intricate operation environment. The analysis of the influence of rain on atmospheric CV-MDI-QKD is the basis to ensure the normal operation of the protocol under raining conditions, which also provides the support for the transmission and occupation of future battlefield information.

The beam distortion and deflection caused by rain are exceedingly minor. The effect of rain on atmospheric CV-MDI-QKD behaves mainly in the beam energy's attenuation caused by the raindrops induced absorption and scattering. We regard this kind of attenuation as rain extinction. In accordance with the empirical formula, the extinction, rainfall intensity and transmission distance are related to each other by[29]

$$\chi_{\text{ext}} = \exp(-210 I_{\text{rain}}^{0.74} L). \tag{17}$$

The size of raindrop is closely related to the intensity of rainfall. The rainfall per unit time is called rainfall intensity. According to raindrop sizes' distribution of Laws–Parsons, the expression of rainfall intensity can be obtained as follows:[30]

$$I_{\text{rain}} = \frac{6\pi N(D) D^3 V(D)}{10^4 m(D)}, \tag{18}$$

where D is the diameter of raindrop, $N(D)$ is the number of raindrops $N(D) = 10^5$, $V(D)$ is the terminal velocity of raindrop, in this paper, we set it to be 9 m/s, and $m(D)$ is the percentage of volume $m(D) = 1$.

Figure 4 illustrates the relationship between raindrop diameter and extinction coefficient. As can be seen from the figure $\chi_{\text{ext}} \in [0, 1]$, the extinction coefficient decreases with the increase of raindrop diameter.

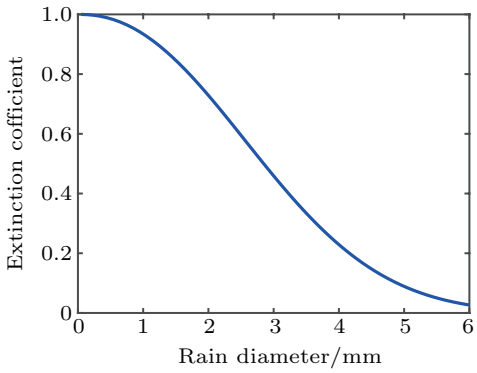

Fig. 4. Relation between extinction coefficient and raindrop diameter.

In practical scene, the diameter of raindrop is positively correlated with rainfall intensity. However, real-time monitoring of rainfall intensity is easier than real-time monitoring of raindrop diameter. Therefore, the extinction coefficient caused by rain can be evaluated by combining rainfall intensity and raindrop diameter, and then the performance of CV-MDI-QKD in rainy weather can be described. Combining the atmospheric CV-MDI-QKD beam deflection model given in the above Section and considering the effect of rainfall on atmospheric CV-MDI-QKD, we can write the transmittance as follows:

$$T_{\text{rain}} = \chi_{\text{ext}} T_1 P(T_1). \tag{19}$$

The panel in Fig. 5 shows the relationship between the secret key rate and the deflection distance. Meanwhile, the diameter of raindrop under rainfall condition is given. The deflection variances are set to be $\sigma^2 = 2.9a$, $\sigma^2 = 14a$, and $\sigma^2 = 64a$ respectively. It is clear from the graph that in the increase of deflection distance, the secret key rate dwindles gradually. Moreover, the larger the diameter of raindrop, the smaller the secret key rate is. The secret key rate varies with the variance of beam deflection. As shown in the figure, the larger the variance, the smaller the secret key rate is. That is because the fluctuation of beam becomes violent with the increase of variance.

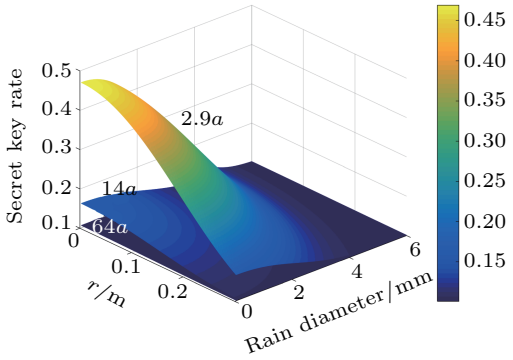

Fig. 5. Relation among secret key rate, deflection distance and raindrop diameter under raininjg condition. The deflection variances are chosen as $\sigma^2 = 2.9a$, $\sigma^2 = 14a$, and $\sigma^2 = 64a$, randomly.

In addition, the distance of transmission is important for the performance of atmospheric CV-MDI-QKD, therefore, we simulate the relationship between the raindrop diameter and secret key rate. Figure 6 gives the simulation results. It is obvious that the secret key rate decreases with transmission distance increasing. What is more, as the raindrop radius increases, the key rate decreases. When the raindrop diameter increases to $D = 3$ mm, the secret key rate drops sharply.

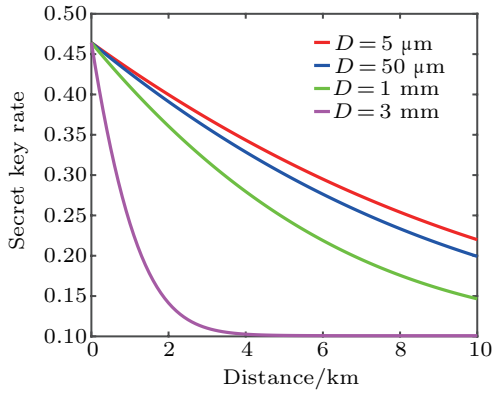

Fig. 6. Plots of secret key rateversus distance under different rain diameters, where $D = 5$ μm, $D = 50$ μm, $D = 1$ mm, $D = 3$ mm.

4. Effects of fog on atmospheric CV-MDI-QKD

Fog is composed of a large number of small droplets suspending in the air. Water droplets floating in the air make the visible distance shorter. When the visible distance is less than 1 km, it is called fog.[31,32] When conducting quantum communication is carried out in foggy weather, the fog can greatly attenuate the beam, which eventually degrades the performance of the protocol, and even causes communication to interrupt in severe cases. The influence of fog droplets on light is mainly reflected in extinction effect, that is, absorption and scattering of light. Extinction effect is primarily related to fog radius and visibility. In this section, the effects of fog on CV-MDI-QKD are analyzed by utilizing the characteristics of fog and Mie scattering theory.

When the particle size is much smaller than the wavelength, the beam scattering can be analyzed by Rayleigh scattering. Usually, the scattering of visible light by atmospheric molecules is known as Rayleigh scattering. When the size of the particle is approximate to the wavelength, the problem of scattering can be treated with Mie scattering theory. Mie scattering theory is established by Mie when studying scattering of metal particles. The theory of Mie scattering is based on the electromagnetic properties of light, in which Maxwell equations is used to present the effects of particles on light scattering.[24,25] Next we will brief the Mie scattering theory on fog.

The case of an isotropic homogeneous spherical particle is considered. The electric field components of the incident wave in the vertical and parallel scattering planes are connected with the corresponding components of the incident beam via the scattering matrix,[21] and described below.

$$\begin{bmatrix} E_{\mathrm{V}}^{S} \\ E_{\mathrm{H}}^{S} \end{bmatrix} = \frac{\exp(\mathrm{i}kr)}{-\mathrm{i}kr} \begin{bmatrix} S_1 & S_3 \\ S_4 & S_2 \end{bmatrix} \begin{bmatrix} E_{\mathrm{V}}^{i} \\ E_{\mathrm{H}}^{i} \end{bmatrix}, \tag{20}$$

where $k = 2\pi/\lambda$, with λ being the incident wave length and $\lambda = 550$ nm in this paper,and S_i is the scattering matrix whose value is determined by the particle shape, scale and refractive index. Due to the symmetry of spherical particles, $S_3 = 0$ and $S_4 = 0$. After a complex solution S_1 and S_2 are expressed as follows:[21]

$$\begin{aligned} S_1 &= \sum_{n=1}^{\infty} \frac{2n+1}{n(n+1)} [a_n \pi_n + b_n \tau_n], \\ S_2 &= \sum_{n=1}^{\infty} \frac{2n+1}{n(n+1)} [b_n \pi_n + a_n \tau_n], \end{aligned} \tag{21}$$

where π_n and τ_n is the coefficients of Scattering angel, with $\pi_n = \mathrm{P}_n^{(1)}(\cos\theta)/\sin\theta = \mathrm{d}\mathrm{P}_n(\cos\theta)/\mathrm{d}(\cos\theta)$ and $\tau_n = \mathrm{d}\mathrm{P}_n^{(1)}(\cos\theta)/\mathrm{d}(\cos\theta)$,with $\mathrm{P}_n^{(1)}(X)$ being the first kind of Legendre function; a_n and b_n are the coefficients of the Mie scattering:

$$\begin{aligned} a_n &= \frac{\psi_n(x)\psi_n'(y) - m\psi_n'(x)\psi_n(y)}{\xi_n(x)\psi_n'(y) - m\xi_n'(x)\psi_n(y)}, \\ b_n &= \frac{m\psi_n(x)\psi_n'(y) - \psi_n'(x)\psi_n(y)}{m\xi_n(x)\psi_n'(y) - \xi_n'(x)\psi_n(y)}, \end{aligned} \tag{22}$$

where $\psi_n(X) = \sqrt{\pi X/2}\,\mathrm{J}_{n+1/2}(X)$, $\xi_n(X) = \sqrt{\pi X/2}\mathrm{H}_{n+1/2}(X)$, $\mathrm{J}_{n+1/2}(X)$ and $\mathrm{H}_{n+1/2}(X)$ are the first kind of semi-integral order Bessel function and Hankel function of the second kind of semi-integral order respectively; $\psi_{\mathrm{n}}'(X)$ and $\xi_n'(X)$ are the derivatives of $\psi_n(X)$ and $\xi_n(X)$ respectively; m is the refractive index of fog droplet and $m = 1.33 + \mathrm{i}0.003$.

The extinction efficiency factor caused by fog droplet is as follows:[21]

$$Q_{\mathrm{ext}} = \frac{\lambda^2}{2\pi} \sum_{n=1}^{\infty} (2n+1)\Re(a_n + b_n). \tag{23}$$

The extinction coefficient of fog can be obtained from Mie scattering theory and expressed as

$$\beta_{\mathrm{ext}} = \pi r_{\mathrm{fog}}^2 Q_{\mathrm{ext}} N_{\mathrm{fog}}, \tag{24}$$

where r_{fog} is the radius of fog droplet, N_{fog} is the distribution Function of fog droplet[33,34] and given as

$$N_{\mathrm{fog}} = c r_{\mathrm{fog}}^2 \exp(-d r_{\mathrm{fog}}), \tag{25}$$

with $c = \frac{9.781}{v_{\mathrm{fog}}^6 W_{\mathrm{fog}}^5} 10^{15}$ and $d = \frac{1.304}{v_{\mathrm{fog}} W_{\mathrm{fog}}} 10^4$ are the parameters to determine the fog droplet spectrum shape, $v_{\mathrm{fog}} = 100$ m and $W_{\mathrm{fog}} = 0.0156 v_{\mathrm{fog}}^{-1.43}$ being visibility and moisture content of fog, respectively.

For atmospheric CV-MDI-QKD, beam extinction means that the transmittance decreases with the increase of extinction coefficient and transmission distance. The transmittance can be expressed as[6]

$$T_{\mathrm{fog}} = \mathrm{e}^{-\beta_{\mathrm{ext}} L}. \tag{26}$$

Figure 7 shows the relationship between droplet radius and transmittance under Mie scattering theory where the distance of transmission is 10 km. As can be seen from the figure, the larger the droplet radius, the smaller the transmittance will be. Besides, when the radius of droplet approaches to 8, it quickly drops to 0. As the radius of fog drop increases, the concentration of fog increases gradually, which will lead to more serious extinction effect of beam.

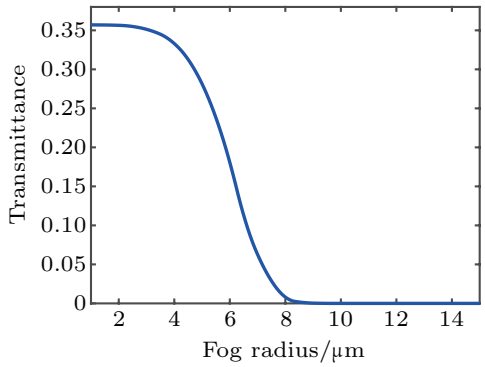

Fig. 7. Relation between droplet radius and transmittance under Mie scattering theory.

Combining the extinction effect of fog droplets with the atmospheric CV-MDI-QKD model, the influence of fog on atmospheric CV-MDI-QKD can be considered comprehensively. Figure 8 shows the relationship between secret key rate and distance. We can find that the distance of transmission has a negative effect on key rate. Like the attenuation effect of raindrops, when the radius of fog drop increases, the key rate decreases. When the droplet radius is relatively large, the secret key rate decreases sharply as the distance of transmission increases.

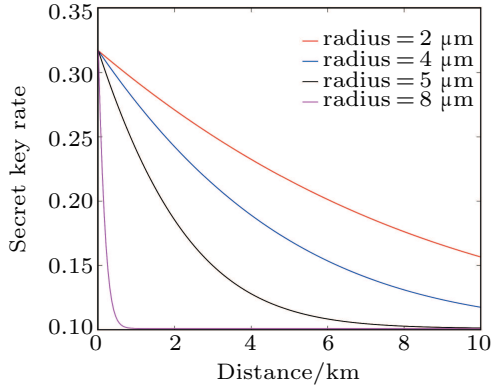

Fig. 8. Plots of secret key rate *versus* distance under diverse radius, where the radius are 2 μm, 4 μm, 5 μm, and 8 μm, respectively.

The relation among secret key rate, deflection distance and droplet radius in foggy environment is obtained in Fig. 9. It can be seen from the figure that the secret key rate decreases with the increase of droplet radius and deflection distance. Moreover, the secret key rate varies with the deflection variance: the smaller the deflection variance, the larger the secret key rate is. As a common weather phenomenon, the emergence of fog even determines whether communication can be established. In the specific battlefield environment, it is necessary to consider fog when trying to build a secret key transmission platform. The relationship between droplet radius and protocol performance is used to evaluate the security and feasibility of the protocol, which lays a foundation for studying the influence of similar weather on CV-MDI-QKD.

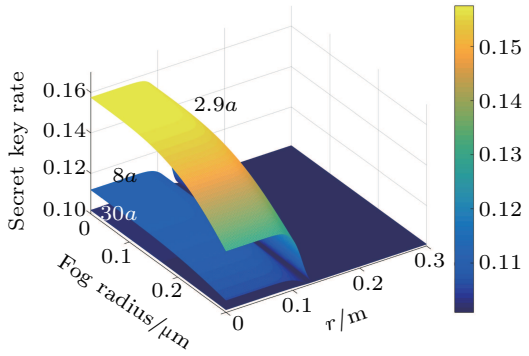

Fig. 9. Relation among secret key rate, deflection distance, and droplet radius in foggy environment, where the variance of deflection is $\sigma^2 = 2.9a$, $\sigma^2 = 8a$, and $\sigma^2 = 30a$, respectively.

5. Conclusions and perspectives

The weather condition is one of the important factors affecting atmospheric QKD in practical application, which cannot be neglected due to the attenuation effect on transmission of beam. In this paper, the variation of atmospheric CV-MDI-QKD performance in rainy weather and foggy weather are analyzed. Under rainy condition, we simulate the effects of CV-MDI-QKD on atmospheric CV-MDI-QKD based on rainfall characteristics and beam deflection model. The numerical simulation shows that with the increase of deflection distance, the secret key rate decreases gradually, and the larger the diameter of raindrops, the smaller the secret key rate is. Under diverse deflection variances of beam, the secret key rate varies. Besides, when the variance is larger, the secret key rate is smaller. In foggy environment, combined with the characteristics of fog and based of Mie scattering theory and atmospheric CV-MDI-QKD model, the influence of fog on atmospheric CV-MDI-QKD is analyzed. In general, fog exerts a negative influence on communication. The numerical simulation results demonstrate that the secret key rate decreases with the increase of droplet radius and deflection distance, and the secret key rate varies with deflection variance: the smaller the deflection variance, the larger the key rate is. In addition, as the distance of transmission increases, the secret key rate drops sharply, especially when the raindrop or fog droplet is large. Our work can provide support and help for the successful establishment of key in future actual field environment, which is urgently needed for secure communication.

References

[1] Bennett C H 1992 *Phys. Rev. Lett.* **68** 3121
[2] Ma X C, Herbst T, Scheidl T, *et al.* 2012 *Nature* **489** 269

[3] Ma H X, Bao W S and Li H W 2016 *Chin. Phys. B* **25** 080309
[4] Huang D, Fang J and Zeng G H 2013 *Chin. Phys. Lett.* **30** 114209
[5] Guo Y, Su Y, Huang D, *et al.* 2019 *Chin. Phys. B* **28** 010305
[6] Wang S Y, Huang P and Zeng G H 2018 *New J. Phys.* **20** 083037
[7] Miao E L, Han Z F, Guo G C, *et al.* 2005 *New J. Phys.* **7** 215
[8] Bourgoin J P, *et al.* 2013 *New J. Phys.* **15** 023006
[9] Paterson C 2005 *Phys. Rev. Lett.* **94** 153901
[10] Berman G P, Chumak A A, *et al.* 2006 *Phys. Rev. A* **74** 013805
[11] Chumak O O, Baskov R A, *et al.* 2016 *Phys. Rev. A* **93** 033821
[12] Semenov A, Töppel F, Vasylyev D Y, *et al.* 2012 *Phys. Rev. A* **85** 013826
[13] Mori S, Marzano F S, *et al.* 2015 *Appl. Opt.* **54** 6787
[14] Vasylyev D Y, Semenov A A, Vogel W, *et al.* 2017 *Phys. Rev. A* **96** 043856
[15] Ma X C, *et al.* 2014 *Phys. Rev. A* **89** 042335
[16] Zhang Y C, *et al.* 2014 *Phys. Rev. A* **90** 052325
[17] Pirandola S, Ottaviani C, Spedalieri G, *et al.* 2015 *Nat. Photon.* **9** 397
[18] Ma H X, Huang P, Bai D Y, Wang S Y, Bao W S and Zeng G H 2018 *Phys. Rev. A* **97** 042329
[19] Hosseinidehaj N and Malaney R 2017 *Quantum Inf. Comput.* **17** 361
[20] Hosseinidehaj N, Malaney R, *et al.* 2015 *Phys. Rev. A* **91** 022304
[21] Wang Y, Fan C, Wei H, *et al.* 2015 *Laser Beam Propagation and Applications Through the Atmosphere and Sea Water* (Beijing: National Defense Industry Press)
[22] Wiscombe W, *et al.* 1980 *Appl. Opt.* **19** 001505
[23] Hansen J E, Travis L D, *et al.* 1974 *Space. Sci. Rev.* **16** 527
[24] Mie G 1908 *Ann. Phys.* **330** 377
[25] James A Lock and Gérard Gouesbet 2009 *J. Quantum Spectrosc. Radiat. Transfer* **110** 800
[26] Vasylyev D Y, Semenov A A, Vogel W, *et al.* 2012 *Phys. Rev. Lett.* **108** 220501
[27] Guo H, Li Z Y, Peng X, *et al.* 2016 *Quantum Cryptography* (Beijing: National Defense Industry Press)
[28] Agrest M M and Maximov M S 1971 *Theory of Incomplete Cylindrical Function and Their Application* (Berlin: Springer)
[29] Uijlenhoet R, Cohard J M and Gosset M 2011 *J. Hydrometeor.* **12** 955
[30] Wolf D, David A, *et al.* 2001 *Radio Sci.* **36** 639
[31] Taylor G I, *et al.* 2007 *Q. J. Roy. Meteor. Soc.* **133** 85
[32] Emmons G, Montgomery R B, *et al.* 2010 *J. Meteor.* **4** 207
[33] Mitchell D L, *et al.* 2000 *J. Atm. Sci.* **57** 1311
[34] Gebhart M, Leitgeb E, Muhammad S S, *et al.* 2005 *Proceedings of SPIE — The International Society for Optical Engineering* **5891**